


## Article

# Alkali-Activated Copper Slag with Carbon Reinforcement: Effects of Metakaolinite, OPC and Surfactants

Patrick Ninla Lemougna<sup>1,2,3</sup> , Guillermo Meza Hernandez<sup>1,2</sup> , Nicole Dilissen<sup>1,4</sup>, Felicite Kingne<sup>1</sup>, Jun Gu<sup>1</sup> and Hubert Rahier<sup>1,\*</sup> 

- <sup>1</sup> Research Group Sustainable Materials Engineering (SUME), Lab of Physical Chemistry and Polymer Science (FYSC), Vrije Universiteit Brussel, Pleinlaan 2, 1050 Brussels, Belgium; patrick.ninla.lemougna@vub.be or lemougna@yahoo.fr (P.N.L.); guillermo.meza.hernandez@vub.be (G.M.H.); nicole.dilissen@vub.be (N.D.); felicite.kingne.kingne@vub.be (F.K.); jun.gu@vub.be (J.G.)
- <sup>2</sup> Strategic Initiative Materials in Flanders (SIM), 9052 Zwijnaarde, Belgium
- <sup>3</sup> Department of Minerals Engineering, School of Chemical Engineering and Mineral Industries (EGCIM), University of Ngaoundere, Ngaoundere P.O. Box 454, Cameroon
- <sup>4</sup> Buildwise, Avenue P Holoffe 21, 1342 Limelette, Belgium
- \* Correspondence: hubert.rahier@vub.be

## Highlights:

### What are the main findings?

- Copper slag can be upcycled in alkali-activated carbon fabric-based composites;
- A 20 wt.% metakaolinite substitution of copper slag increases reaction heat and mechanical properties;

### What is the implication of the main finding?

- Low reactivity at 20 °C, but instantaneous at 80 °C with K-solution SiO<sub>2</sub>/K<sub>2</sub>O of 2.25;
- Composites with an elastic modulus of 19 GPa and flexural strength of 88 MPa.



**Citation:** Lemougna, P.N.; Hernandez, G.M.; Dilissen, N.; Kingne, F.; Gu, J.; Rahier, H. Alkali-Activated Copper Slag with Carbon Reinforcement: Effects of Metakaolinite, OPC and Surfactants. *Appl. Sci.* **2024**, *14*, 2081. <https://doi.org/10.3390/app14052081>

Academic Editor:  
Patrick A. Fairclough

Received: 20 January 2024  
Revised: 17 February 2024  
Accepted: 27 February 2024  
Published: 1 March 2024



**Copyright:** © 2024 by the authors. Licensee MDPI, Basel, Switzerland. This article is an open access article distributed under the terms and conditions of the Creative Commons Attribution (CC BY) license (<https://creativecommons.org/licenses/by/4.0/>).

**Abstract:** Copper slag is an industrial residue with a large unutilized fraction. This study presents the development of alkali-activated composites from a copper slag named Koranel<sup>®</sup>. The effects of metakaolinite, ordinary Portland cement (OPC) and surfactants were investigated. The reactivity of Koranel with potassium silicate solutions with molar ratio  $R = \text{SiO}_2/\text{K}_2\text{O}$  varying from 1 to 2.75, with 0.25 intervals, was investigated using isothermal calorimetry. The reactivity was relatively low at 20 °C; the reaction started after a few hours with a low silica modulus, to several weeks with the highest silica modulus. The substitution of Koranel by OPC (5 wt.%) or by metakaolinite (10–20 wt.%), both led to higher reaction heat and rate; meanwhile, the addition of 2 wt.% polyethylene glycol/2-methyl 2,4 pentanediol delayed the reaction time in the system containing metakaolinite. Raising the curing temperature from 20 °C to 80 °C shortened the setting time of the low reactive systems, from several days to almost instantaneous, opening perspectives for their application in the production of prepreg composite materials. The use of carbon fabric as reinforcement in the alkali-activated matrix led to composite materials with flexural strength reaching 88 MPa and elastic modulus of about 19 GPa—interesting for engineering applications such as high-strength lightweight panels.

**Keywords:** copper slag; alkali-activated materials; laminate composite; elastic modulus; flexural strength

## 1. Introduction

Steel-reinforced concrete is the most important composite material used for structural applications in civil engineering [1,2]. However, textile-reinforced concretes (TRCs) have attracted interest for many civil engineering applications, owing their advantages over steel reinforcement, including more design freedom, limited use of cementitious matrices, and improved resistance to corrosion [1,3–5]. The TRC is a kind of concrete composite

mainly made of a woven fabric embedded as reinforcement in a finely grained cementitious matrix [1,3,6,7]. The fabric (“a manufactured planar textile structure made of fibers and/or yarns assembled by various means such as weaving, knitting, tufting, felting, braiding, or bonding of webs to give the structure sufficient strength and other properties required for its intended use”) [1] could be made of different type of materials including carbon, basalt, aramid, polyethylene (PE), polypropylene (PP), poly-vinyl-alcohol (PVA), glass and also cellulose-based natural fiber [4,8,9].

Ordinary Portland cement (OPC) has been commonly used as binder for cementitious matrices for TRC [2,3,10]. Research activities on other binder types, including alkali-activated materials (AAMs), have been performed to address sustainability issues or improve specific TRC properties [3,11–13]. AAMs are materials enclosing binder systems resulting from the reaction of a solid or dissolved alkali metal source with a solid silicate powder, and they have the potential to reduce up to 70–80% CO<sub>2</sub> emissions compared with the cement industry if optimally formulated [13–15].

It is worth noting that the development of AAMs could also offer the possibility for upcycling industrial residues [16,17]. For instance, about 2.2 tons of copper slag (such as Koranel slag) are generated per ton of copper produced [18,19]. Hence, the production of TRC from a cementitious matrix containing Koranel slag will contribute to waste management.

Potential applications of TRC include facing and sandwich panels; thin-walled lightweight elements; lightweight constructions and complex civil engineering structures; repair of existing buildings and constructions; fire resistance; and high temperature performance materials [5,20–22]. However, at variance to textile/organic resin-based composites, no prepreg with mineral matrix exists. Prepreg can be prepared and stored for a long period at low temperature and sold before the final shaping. Mineral-based matrices such as AAMs are generally subjected to relatively rapid setting time at ambient temperatures, limiting their flexibility. The development of a mineral-based matrix for TRC with storage flexibility comparable to that of organic resin will widen their potential applications.

The aim of this study is the development of an alkali-activated matrix based on Koranel slag for laminated TRC composites with woven carbon fiber reinforcement. The reactivity of Koranel with potassium silicate solutions having a silica-to-potassium molar ratio ( $R = \text{SiO}_2/\text{K}_2\text{O}$ ) varying from 1 to 2.75, with 0.25 intervals, was investigated to select the modulus, giving a reasonable open pot life of several hours at room temperature. This will allow the use of such a matrix in an impregnation bath for several hours without the need to refresh the mixture. The impregnated textile will also be stable for some hours allowing the handling, for instance, to drape in a mold. Isothermal calorimetry at 20 °C was used to select a suitable alkaline solution with low reactivity at ambient temperature. If such a matrix has high reactivity above ambient temperature (50–100 °C), the composite could be hardened in the mold in one hour, for instance, as is the case for organic resin textile composites. Differential scanning calorimetry was used to investigate the temperature at which the selected matrix started to react with a reasonable rate. The effect of 10–20 wt.% metakaolinite, 5 wt.% OPC and surfactant was also investigated on the reaction heat and rheology. Indeed, metakaolinite is a finer precursor which could facilitate fiber impregnation by the matrix. Some surfactants were already proposed in the literature about alkali activation, although for different reasons than making composites [23]. Finally, the bending strength and elastic modulus of the composites prepared with carbon fabric and formulated compositions were assessed, as well as the elastic modulus of both matrix and composite upon heating until 700 °C.

## 2. Materials and Methods

### 2.1. Materials

The copper slag used in this study was Koranel<sup>®</sup> from Aurubis Beerse nv in Beerse, Belgium, with 2600 cm<sup>2</sup>/g Blaine surface. The Blaine was measured with an air permeability apparatus as described in EN 196-6:2018 [24]. The particle size distributions of the Koranel slag, metakaolinite and OPC were determined by a laser particle size analyzer (Beckman

Coulter LS 13320, Pasadena, CA, USA) (Figure 1a). X-ray powder diffraction (XRD) spectra of the slag were taken by a Bruker D2 Phaser, Karlsruhe, Germany, in the 6–70° 2 $\theta$  range using Cu K $\alpha$  radiation (voltage 40 kV and current 40 mA), a step size of 0.02° and scan speed of 0.5 s/step. The XRD pattern shows that the material is mainly amorphous (Figure 1b), with few crystalline features ascribed to Fayalite, Fe<sub>2</sub>SiO<sub>4</sub> (PDF 34-0178), Ankerite, Ca (Fe, Mg)(CO<sub>3</sub>)<sub>2</sub> (PDF 33-0282), and Fe-rich spinel, (Al,Fe)<sub>2</sub>O<sub>4</sub> (PDF 21-0540) (see also [25]).

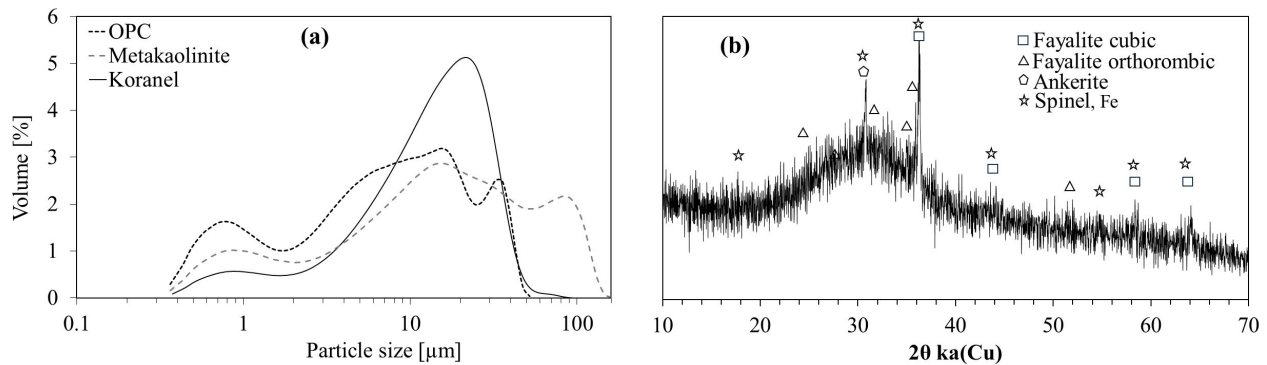


**Figure 1.** (a) Particle size distribution of Koranel<sup>®</sup> with Blaine 2600 cm<sup>2</sup>/g, adapted from [25]; (b) XRD diffraction pattern of Koranel<sup>®</sup> with Blaine 2600 cm<sup>2</sup>/g.

The metakaolinite (MK) used in this study is Argical<sup>TM</sup>-M 1000 from IMERYS Fused Minerals, Paris, France. The ordinary Portland cement used was of CEM I 52.5 R from CBS Heidelberg cement group, Heidelberg, Germany. The chemical composition of Koranel, OPC and metakaolinite, as determined by X-ray fluorescence (PW 2400 Philips) on powder, is presented in Table 1. The d<sub>10</sub>, d<sub>50</sub> and d<sub>90</sub> of Koranel were respectively 2.51 µm, 13.22 µm and 27.87 µm. These values were, respectively, 0.87 µm, 7.88 µm and 30.40 µm for OPC and 1.31 µm, 16.01 µm and 80.57 µm for the metakaolinite. The 2-Methyl 2,4-Pentanediol and the Polyethylene Glycol 600 (PEG 600) used as surfactant were from Sigma Aldrich, Overijse, Belgium. The potassium hydroxide (Sigma Aldrich; 85 wt.% purity) and potassium silicate solution (Silmaco, Lanaken, Belgium) were used for the preparation of the activating solution. The potassium silicate solution was made of 27.22 wt.% SiO<sub>2</sub>, 15.01 wt.% K<sub>2</sub>O and 57.3 wt.% H<sub>2</sub>O, with a molar ratio (R = SiO<sub>2</sub>/K<sub>2</sub>O) of 2.84 and density of 1.424 g/cm<sup>3</sup> at 20 °C. The potassium hydroxide was used to adjust the ratio in the solution. For instance, for 100 g of the potassium silicate solution, the amounts of KOH added to achieve the SiO<sub>2</sub>/K<sub>2</sub>O molar ratios of 1, 1.5, 2 and 2.25 were, respectively, about 38.7 g, 18.8 g, 8.9 g and 5.5 g. This corresponded to an addition of 32.9 g of pure KOH for the solution with R = 1, 15.9 g for R = 1.5, 7.5g for R = 2 and 4.7 g for R = 2.25; one hundred (100) g of these solutions contained a total mass of water (including water from dissolved KOH) of 44.4 g, 50.2 g, 53.9 g and 55.3 g, respectively. The properties of the 200 g/m<sup>2</sup> carbon fabric used (Fibermax Composite, London, UK) are presented in Table 2. Carbon fiber was chosen due to its high specific strength and its relatively chemical and thermal stability [26]. This allows the composite properties to be relatively stable over time, since no fiber degradation is expected due to the alkaline nature of the alkali-activated matrix.

**Table 1.** Normalized chemical composition in wt.% by XRF analyses for Koranel (K), metakaolinite (MK) and OPC. \* Includes small amounts that are <0.1 wt.%. \*\* Loss on ignition at 950 °C.

Samples	SiO <sub>2</sub>	Al <sub>2</sub> O <sub>3</sub>	Fe <sub>2</sub> O <sub>3</sub>	CaO	MgO	Cr <sub>2</sub> O <sub>3</sub>	K <sub>2</sub> O	TiO <sub>2</sub>	P <sub>2</sub> O <sub>5</sub>	SO <sub>3</sub>	Others *	LOI **
K	26.6	9.5	57.4	2.8	0.9	0.7	0.2	0.2	0.8	0.9	0.0	-
MK	51.9	40.9	1.7	0.1	0.1	0	1	2.1	0	0	0.3	1.9
OPC	19.7	5.2	3.0	64.2	1.7	0	0	0.3	0	2.7	1.6	1.6

**Table 2.** Properties of individual carbon fiber from Fibermax Composite.

	Area Density (g/m <sup>2</sup> )	Tensile Strength (MPa)	Tensile Modulus/E-Modulus (GPa)	Elongation at Break (%)
Carbon (Plain woven)	200	4410	235	1.9

## 2.2. Sample Preparation

To select the appropriate activating solution with low reactivity at ambient temperature and relatively high reactivity at 50–100 °C, a series of experiments with different potassium silicate solutions were performed. Different silica to potassium moduli ( $R = \text{SiO}_2/\text{K}_2\text{O}$  molar ratio), ranging from 1 to 2.75, with 0.25 intervals, were investigated with an L/S of 0.55, with L being the silicate solution. The prepared solutions were stored for 1 day in the laboratory environment for further equilibration. The dry components (Koranel (K) + metakaolinite (MK) + Portland cement (OPC)) and liquid components (prepared potassium silicate solution and 2-methyl 2,4-pentanediol (“m”) or polyethylene glycol (“p”)) were first mixed separately; then, both liquid and solid components were mixed using an electric laboratory stirrer at a speed of 1000 rpm for 5 min to obtain a homogeneous slurry. The details on the formulated matrices for the preparation of the composite materials are presented in Table 3.

**Table 3.** Composition of the different matrices used for the preparation of the laminates with Koranel (K), metakaolinite (MK), Portland cement (OPC), 2-methyl 2,4-pentanediol (m) or polyethylene glycol (p). Sample names are composed of the letters mentioned between brackets and corresponding number of wt.% of the solid. \* Discarded due to short setting time.

Sample Codes	Koranel (g)	Potassium Silicate Solution R = 2.25 (g)	Metakao-Linite (g)	OPC (g)	2-Methyl 2,4-Pentanediol (g)	PEG 600 (g)
K	100	55	-	-	-	-
Kp	100	55	-	-	-	2
Km	100	55	-	-	2	-
90K10MK	90	55	10	-	-	-
80K20MK	80	55	20	-	-	-
80K20MKm	80	55	20	-	2	-
80K20MKp	80	55	20	-	-	2
95K5OPC	95	55	-	5	-	-
90K10OPC *	90	55	-	10	-	-

For the composite preparation, a thin layer of about 0.5 mm of alkali-activated matrix was spread on a plastic PET film placed on a wooden mold in a pre-drawn square of  $15 \times 15 \text{ cm}^2$ . The first layer of carbon-woven fabric ( $15 \times 15 \text{ cm}^2$ ) was placed on top of the matrix layer. Thereafter, the carbon fabric was manually wet out (impregnated) with alkali-activated matrix using a roller (1; Figure 2). The process was repeated for 4 layers of the woven fabric and finally, a layer of geopolymer matrix was added; hence, we obtained a composite made of 5 matrix layers and 4 fiber layers (2; Figure 2). Caution was taken to use a minimum amount of matrix to ensure sufficient fiber impregnation with a high fiber volume fraction. Four weights of 5 kg each (3; Figure 2), equivalent of a total force of 196 N, were equally distributed on top of the laminate composites, and cured at 80 °C for 24 h in a conventional oven (4; Figure 2). After the curing period, the samples were cut in composite beams of 2.5 cm width and 14 cm length, then kept for 3 days in a laboratory environment before testing.

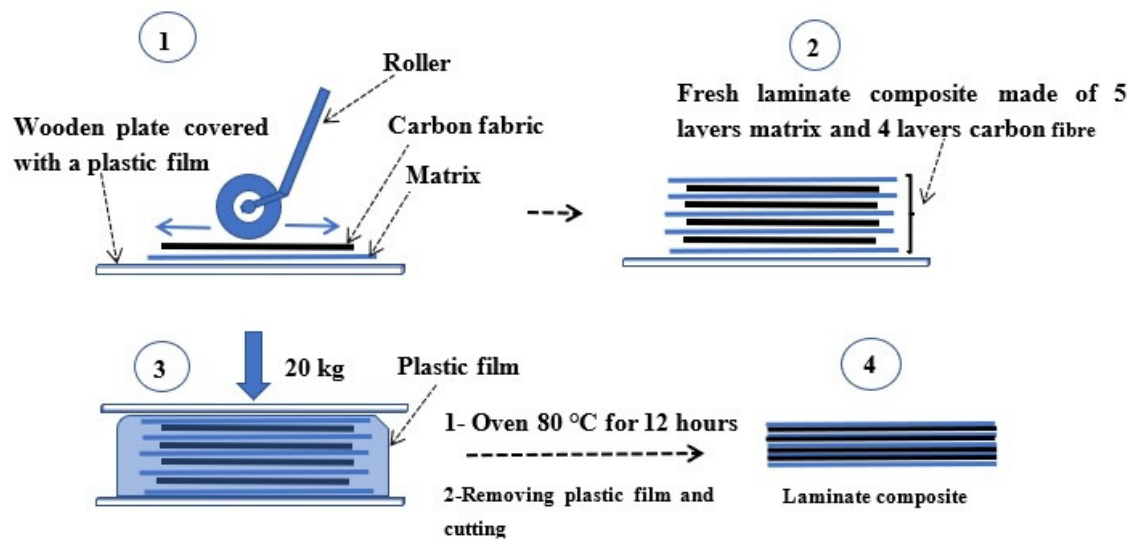


**Figure 2.** Sketch of laminate preparation. For details on the preparation, see text.

For comparative purposes, selected matrices were cast as paste in  $4 \times 4 \times 16 \text{ cm}^3$  molds at once without vibrating and cured at 80 °C for 24 h.

### 2.3. Characterization Methods

#### 2.3.1. Differential and Isothermal Calorimetry

Isothermal (20 °C) calorimetry (TAM Air, TA instruments, New Castle, DE, USA) was performed on 10 g of the solid part mixed with 7 g liquid. Mixing for 2 min at 1600 rpm occurred outside the calorimeter in the ampoule, which was placed within the calorimeter immediately after mixing. The data collection started 45 min after the start of mixing.

Non-Isothermal differential scanning calorimetry (DSC) was performed with a Mettler Toledo DSC822e, USA, using nitrogen ( $\text{N}_2$ , 100 mL/min) as a purge gas. Freshly mixed sample, 25 mg as seen in Table 3, was placed into a platinum crucible and heated from 0 to 250 °C at 5 °C/min to assess the temperature at which the matrix starts to react.

#### 2.3.2. Scanning Electron Microscopy

Scanning electron microscopy was performed on an SEM device (Phenom Benelux Scientific X pro, Nazareth, Belgium) using an acceleration voltage of 5 kV and backscatter electron (BSE) for imaging. The samples were cut and put in the SEM sample holder; no conductive coating was applied. Possible remaining dust on the specimen was removed by compressed air before inserting it into the device.

#### 2.3.3. Rheology

Viscosity analyses were performed at 25 °C with an AR-G2 rotational Rheometer from TA instruments, New Castle, DE, USA, using a cone plate and stainless steel geometry set up with a diameter of 15 cm.

#### 2.3.4. Mechanical Properties

The mechanical testing included compressive strength and elastic modulus. The compressive tests were performed with an Instron 5885H test bench, Darmstadt, Germany. The instrument was equipped with a loadcell of 250 kN, and the tests were executed with a displacement rate of 1 mm/min. The elastic modulus was performed with a Resonalyser device [27], Bytec company, Merksplas, Belgium. This nondestructive method was performed on the samples prior to the flexural and compressive tests. The flexural strength was obtained with three-point bending tests performed with a Tinius Olsen 5ST, Surrey, UK.



### 2.3.5. Fiber Volume Fraction Estimation

The fiber volume fraction influences the mechanical properties and is determined as reported by Messiry [28] as:

$$V_f = \rho_f \times W_f / (\rho_f \times W_f + \rho_m \times W_m)$$

with  $V_f$  as the volume fraction of the fibers,  $W_f$  as the weight of the fibers,  $W_m$  as the weight of the matrix,  $\rho_f$  as the density of the fibers, and  $\rho_m$  as the density of the matrix.

The sketch of the experimental plan is presented in Figure 3.

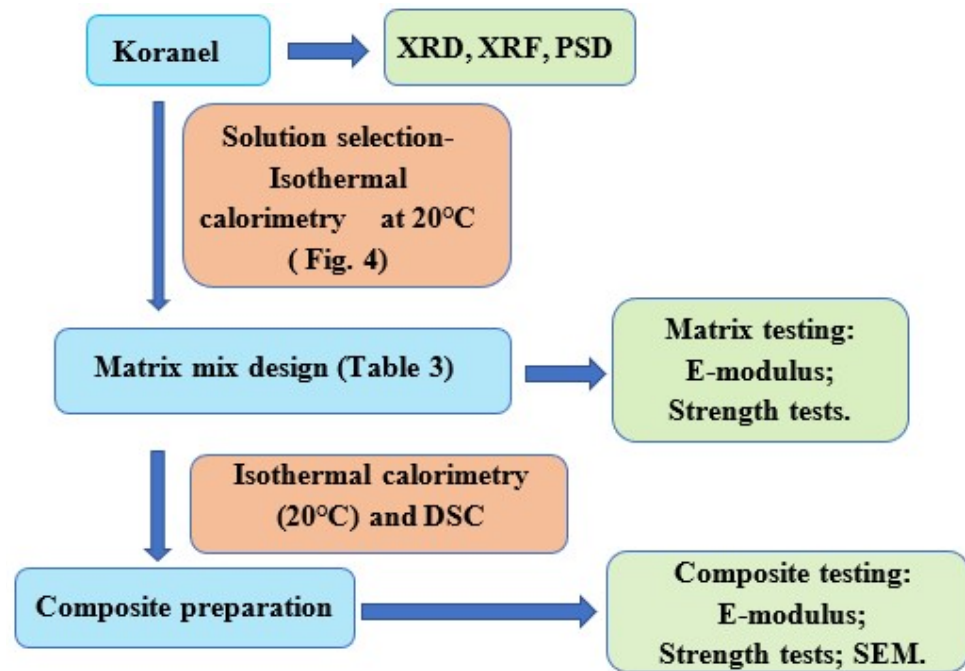


Figure 3. Sketch of the experimental design.

## 3. Results and Discussion

### 3.1. Reactivity of Matrices

#### 3.1.1. Influence of Solution Silica Modulus on Reactivity at Room Temperature

The effect of the silica modulus of the potassium silicate solution on the reaction time was studied with isothermal calorimetry on Koranel (Figure 4). For potassium silicate solutions having a silica-to-potassium molar ratio ( $R$ ) below 1.75, the reaction started earlier than the measurement (i.e., <45 min after mixing) and with a high rate. For  $R = 2.00$ , an induction period of 2 h was observed, and while increasing  $R$ , the induction time becomes 60 h (2.5 days) for  $R = 2.25$  and 350 h (about 2 weeks) for  $R = 2.5$  (Figure 4a). The peak of reaction also becomes broader and lower while increasing  $R$  from 2 to 2.5.

For  $R = 2.25$ , even a double exothermic peak is observed, i.e., one main peak at 3 days and the second smaller bump with maximum at 5.5 days. Such a smaller bump is not observed for  $R = 2$ , likely due to the fast reaction and overlap, and is neither observed for  $R = 2.5$ , likely because it is small and could occur at an even later time than the measurement of 24 days.  $R = 2.25$  thus gives the unique insight into the complex reaction mechanism of potassium silicate-activated Koranel. Two exotherms for certain non-ferrous slags were also observed by others [17] who performed sodium silicate activation. The main peak observed is corresponding to the polymerization reactions [29,30], while the second, smaller and broader exotherm, seems to be depending on the silica content of the activator and is due to a secondary reaction or reorganization of the polymer network [17]. For none of the samples a split in decomposition, polymerization and stabilization was observed, as was described for metakaolinite [31]. The decomposition and polymerization seem to occur in

the same exotherm. More recently, R. Caron [32] defined the steps in alkali activation more precisely as being first a nucleation and growth process, followed by volume contraction due to the polymerization, an induction period, a second nucleation and growth process corresponding to the second exotherm, new volume contraction process, and finally, slow diffusion controls further curing. According to our own insight, the first nucleation has not to be seen as a nucleation for crystals, but occurs as a result of polymerization and densification, comparable to the polymerization of an organic thermoset. An important difference is that no phase boundary, as between crystal and liquid, needs to be formed. The diffusion control occurs because of the formation of a dense layer around and in between the remaining slag particles, rendering the diffusion of ions more difficult than in the initial liquid activator. Although Koranel is an iron silicate (containing a high proportion of iron and silica), and thus chemically different from the slags and metakaolinite for which the mechanisms were described, one can assume that the general steps remain the same but that the products formed are different.

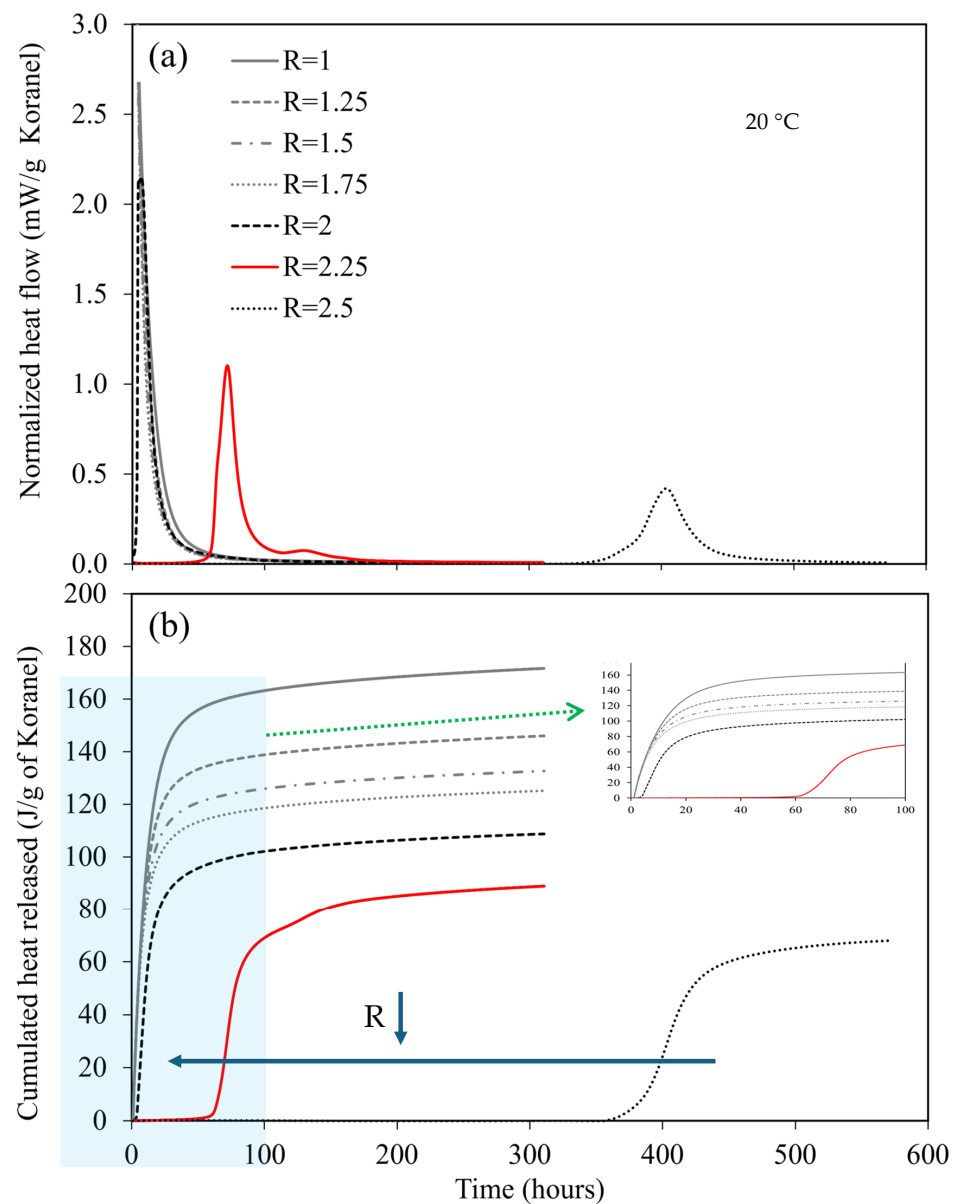


**Figure 4.** Effect of the silica-to-potassium molar ratio ( $R = \text{SiO}_2/\text{K}_2\text{O}$ ) of the activating solution on (a) the normalized heat flow, and (b) the cumulative heat released per gram of solid of alkali-activated Koranel.

For a matrix to be used for textile, sufficient time before setting is needed if we consider a continuous production of several hours from prepared batches of matrix; the low reactivity will then prevent unwanted matrix setting during the production.

The normalized cumulative heat released from the different compositions (Figure 4b) shows that the reaction heat increases with the reduction of R due to the higher concentration of  $\text{OH}^-$  in the alkaline solution; this favors Koranel dissolution and polymerization reactions. However, a higher degree of dissolution is also associated with a faster reaction at room temperature. The matrix with  $R = 2.25$  has therefore an ideal setting time (i.e., 60 h) for the purpose of laminate composite preparation in a production with batches of paste and is used in the following experiments. Its reactivity is low at room temperature but can be increased by increasing the curing temperature, as will be studied further on.

### 3.1.2. Influence of Additives and Koranel Replacement on Reactivity

With the selected activator solution, the influence of surfactants and small amounts of other precursors was investigated. The isothermal calorimetry at 20 °C (Figure 5) of the different compositions (Table 3) shows that the start of the reaction at room temperature differs depending on the composition of the solid phase. The addition of 5 wt.% OPC (brown curve; Figure 5a) decreased the open pot life with a factor of about 3; a sharp exotherm is observed. Meanwhile, the addition of metakaolinite (gray curves; Figure 5a) induced a delay in the appearance of the first exotherm. For the Koranel-based system (black curves; Figure 5a), the addition of surfactants slightly speeds up (2,4 methyl pentanediol) or delays (polyethylene glycol) the reaction; however, with the addition of metakaolinite, the effect of the surfactant was less obvious, a slight broadening of the peak might be observed.

The cumulative heat released (Figure 5b) of the different compositions clearly shows that the addition of OPC and metakaolinite leads to higher reaction heat, the latter being higher for the sample made of 20 wt.% metakaolinite in comparison to those made of 10 wt.% metakaolinite. The cumulative heat released per g of matrix varied from about 85 J/g for the composition made of Koranel to 140 J/g for the composition containing 20 wt.% metakaolinite. The increase from 85 J/g for Koranel to 115 J/g for 90K10MK is rather large, and the replacement of 10 wt.% more of Koranel by MK does not give rise to the same step in heat released, but only to an extra amount of 15 J/g. The cumulative heat released lowers upon the addition of both surfactants to the Koranel system. This was not expected but it shows that they interact chemically during the reaction and this interaction has a more important effect than being pure catalytic. Two evident ways the surfactants can play a role in the reaction rate are: (i) interaction with the surface of the precursor which could lead to a reduced reaction rate due to a reduced effective surface area; and (ii) interaction with the ions in solution, comparable to a chelating effect, although none of the surfactants are ionic, as is usually the case for chelating agents. This effect could also explain a reduction in reaction rate. No explanation was found for the shorter induction period observed for 2,4 methyl pentanediol. The maximum heat flow, thus maximum reaction rate, is for both pastes with surfactants substantially lower, as expected, according to the explanation given. These mechanisms can however not explain the slightly earlier start of the reaction and no other explanation could be found so far. Upon replacement of Koranel with metakaolinite, both surfactants have a different effect. While “p” does not influence the reaction too much, “m” decreases the total heat released substantially, though both had a slightly accelerating effect on the start of the reaction.

For an optimum dosage of alkali in alkali-activated materials from known precursors such as metakaolinite, the added alkali, M, should be enough to compensate the charge balancing of Al; hence, the M/Al molar ratio should be 1 [33]. Considering the chemical composition of Koranel and metakaolinite and the use of potassium silicate solution of  $R = 2.25$  and a liquid-to-solid ratio of 0.7, the molar ratio K/Al in the alkali-activated mixture was 0.88 for matrix 80K20MK (Table 3) made of 20 wt.% metakaolinite and 80 wt.% Koranel. This means the alkaline reagent in matrix 80K20MK is theoretically not in excess for the alkali-activated reaction. Furthermore, for iron-rich slags, iron or iron-bearing



phases in the slag also participate in the formation of the binding phase [14,34]. However, the degree of reaction of most of non-synthetic aluminosilicates is usually not 100% and some relics of the precursors are often evidenced by SEM [35]. Thus, for Fe silicates and Ca silicates, it is not only the K/Al ratio that is important, but other parameters also play a role as other reaction products such as calcium aluminosilicate hydrate (C-A-S-H) are formed. The exact stoichiometry is still not well known and the fact that reaching a 100% conversion with such systems is almost impossible hampers a more in-depth study.

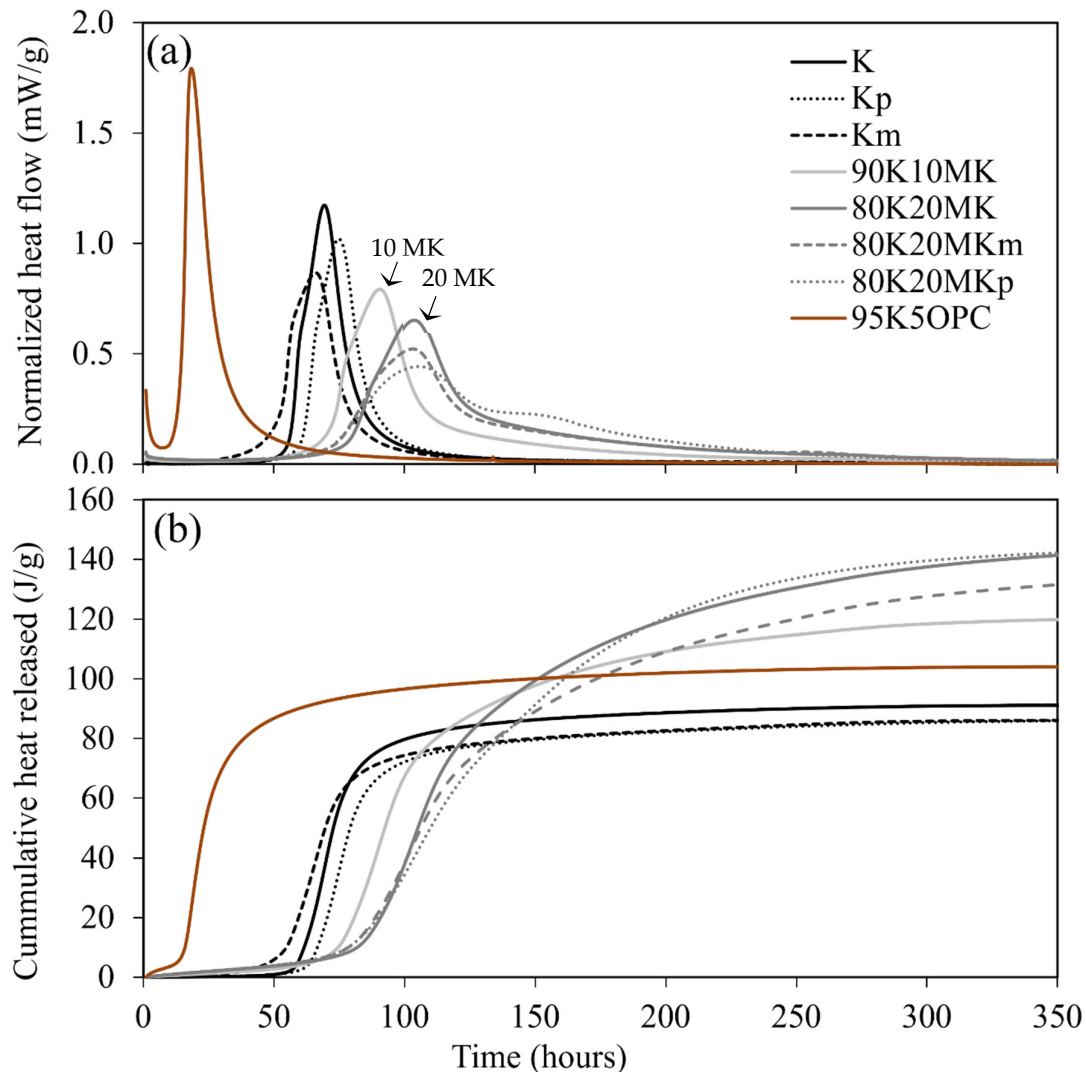


**Figure 5.** (a) Normalized heat flow and (b) cumulative heat released per gram of solid of alkali-activated materials with silicate modulus 2.25 and compositions defined in Table 3. Surfactant p is polyethylene glycol and m is 2-methyl 2,4-pentanediol.

In conclusion, one can state that the replacement of Koranel by OPC speeds up the reaction drastically, thus, the open pot life becomes too short for the application in mind. Replacement of Koranel with metakaolinite enhances the reaction. The addition of surfactants influences the reaction but the effect is limited. In the rest of this paper, the mixture of Koranel and metakaolinite as precursor will be further studied.

### 3.1.3. Reactivity with Increasing Temperature

The next step is to check if the reaction mixtures can set/harden within a time of about one hour at elevated temperature. Here again we have in mind a production method whereby the composite will be shaped and pressed at a higher temperature, as is normally

performed for thermoset-based composites. The DSC trace of composition K with 100 wt.% Koranel as solid (reference composition) and matrix 80K20MK that presented the highest reaction heat due to metakaolinite addition is presented in Figure 6.

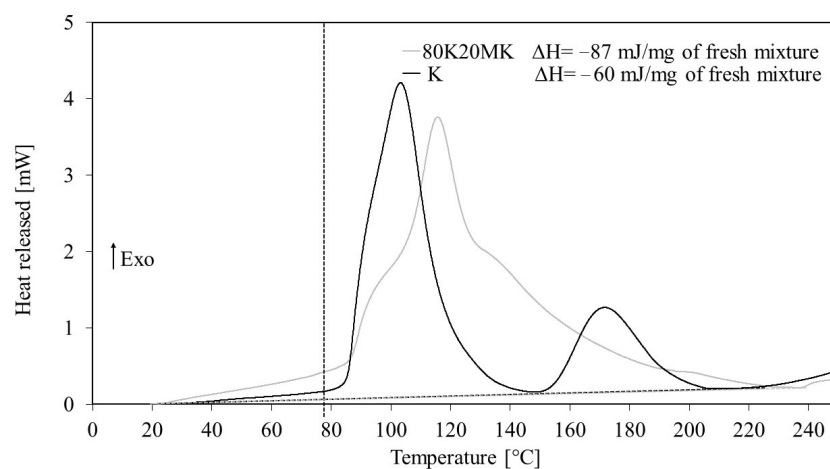


**Figure 6.** DSC curves of matrices K and 80K20MK (See Table 3). K shows two exothermic peaks at 100 °C and 150 °C with total enthalpy of  $\Delta H = -60$  J/g; 80K20MK shows one exothermic peak at 120 °C with two shoulders at 95 °C and 140 °C with  $\Delta H = -87$  J/g.

The reaction of Koranel with the alkaline solution is complex and occurs in two steps as indicated by two successively occurring exothermic peaks in the DSC pattern. The main exothermic reaction starts around 80–85 °C. The addition of 20 wt.% metakaolinite shifts the reaction start to a slightly lower temperature, 75 °C. This shift could be ascribed to the fineness and difference in activation energy of the added metakaolinite. The effect is however opposite to what was observed at 20 °C, where MK slowed down the reaction.

This observation from DSC indicates that 80 °C is a reasonable curing temperature for this matrix based on Koranel. The reaction enthalpies were  $-87$  and  $-60$  J/g for the 80K20MK and K compositions, respectively, or about  $-150$  and  $-103$  J/g of solid for the 80K20MK and K compositions, respectively; this is more or less comparable to the heat released after 2 weeks curing, measured using isothermal calorimetry at 20 °C (Figure 5).

### 3.2. Effect of Surfactants on the Properties of Matrices

#### 3.2.1. Rheology of Fresh Matrices

Surfactants are often used to reduce the amount of water, thus the L/S ratio, given that they reduce the viscosity. They might also have an influence on the wetting of fibers in composites. The effect of two surfactants is discussed here. The effect of 2-methyl 2,4 pentanediol (“m”) and PEG (“p”) on the rheology of the fresh matrices K, 80K20MK<sub>m</sub> and 80K20MK<sub>p</sub> was compared each time with the selected matrix 80K20MK (Figure 7; see Table 3 for matrices).

The substitution of 20 wt.% copper slag by metakaolinite has a special effect on the viscosity (Figure 7a). At low shear rates, a decrease in the thixotropy is observed due to the addition of metakaolinite. This is interesting for the flow of the paste at almost steady conditions, for instance, when a textile is pulled through a bath of matrix. Under those conditions, the thixotropy of the pure Koranel-based matrix hinders a uniform deposition of the matrix on the textile. However, at intermediate shear rates there is no substantial difference between both pastes up to a rate of about 2/s, when the viscosity of the mixture with MK becomes slightly higher than the one without MK. The shear thinning observed at intermediate shear stresses can be related to the alignment of particles. The addition of 2 wt.% 2-methyl 2,4 pentanediol to 80K20MK reduced the viscosity and shear stress slightly up to 1/s (Figure 7b), opposite to polyethylene glycol, for which there is a slight increase in almost the complete studied range of shear rates (Figure 7c).

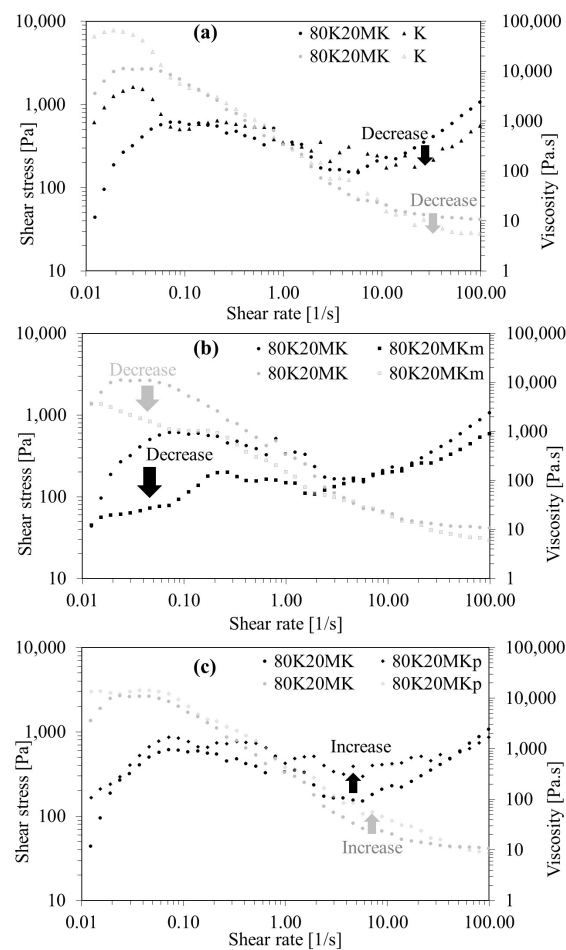


**Figure 7.** Rheology of matrices K (a), 80K20MKm (b) and 80K20MKp (c), all indicated with open dots in comparison with matrix 80K20MK, indicated with filled dots.

In our system, MK thus lowers the thixotropy; the surfactants did not change the rheology to a large extent. Only 2 wt.% 2-methyl 2,4 pentanediol lowered the viscosity in the intermediate range, with maximum a factor of 10. PEG slightly increased the viscosity in the studied composition range.

### 3.2.2. Mechanical Properties of Hardened Matrix Pastes

The effect of 2-methyl 2,4 pentanediol and polyethylene glycol on compressive strength, flexural strength and elastic modulus of 80K20MK is presented in Figure 8. Matrices 100K, 80K20MK, 80K20MKm and 80K20MKp were cured at 80 °C for 24 h with additional post-curing at room temperature for 3 days. Matrix 80K20MK resulted in a compressive strength of 30 MPa, somewhat better than the pure Koranel with the same activator. The addition of 2-methyl 2,4 pentanediol had no effect on the compressive strength; meanwhile, polyethylene glycol contributed to an increase of 35 MPa. The flexural strength for 80K20MK was 0.8 MPa, comparable to the one for pure Koranel. The addition of 2-methyl 2,4 pentanediol tripled the flexural strength to 2.5 MPa and that of polyethylene glycol helped even to reach 4 MPa. This positive effect is also noticeable in the elastic modulus, for which 80K20MK reaches 3 GPa, and 80K20MKm and 80K20MKp reach, respectively, 5.3 and 6.3 GPa in bending, whereas for axial, it reaches 2.5, 4.6 and 6.2. This large effect of surfactants is likely due to their influence on reducing microcrack formation [23], thus posing these surfactants forward as valuable additions for producing high strength lightweight panels. The fact that the compressive strength increases only slightly is because defects are closed upon

compression, while for flexion, a crack means concentration of the force on the edges. Thus, the structure will become stronger if less cracks are formed.

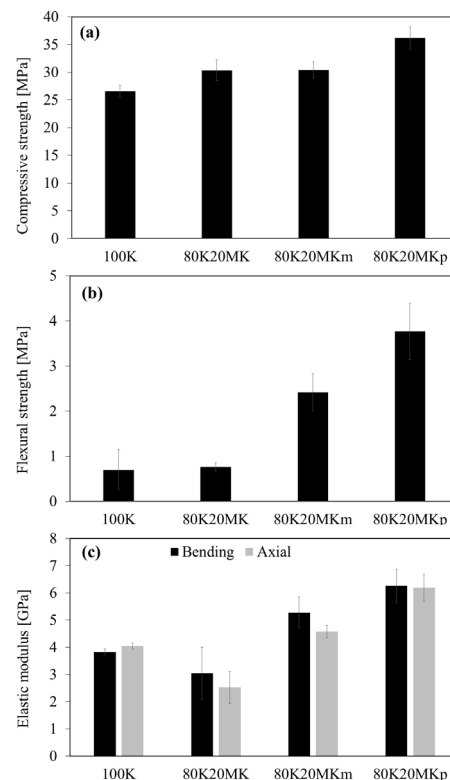


**Figure 8.** (a) Compressive strength, (b) flexural strength and (c) elastic modulus of matrices 100K, 80K20MK, 80K20MKm and 80K20MKp after curing for 1 day at 80 °C and 3 days post-curing at room temperature to compare the effect of 2-methyl 2,4 pentanediol (“m”) and polyethylene glycol (“p”) on these mechanical properties. Both surfactants increased the compressive strength, but the effect is most pronounced on the flexural strength that increases with a factor of about 4.

Compared to some of the literature data [17], a compressive strength of 35 MPa is rather low. The most likely reason is the lower OH<sup>-</sup> concentration or higher modulus of the chosen activating solution, which was beneficial for the lower reaction rate but also leads to a higher fraction of undissolved slag in the hardened alkali-activated slag. The flexural strength of concrete is usually a factor of 8–10 lower than the compressive strength [36]. The flexural strength for the samples without surfactants is thus rather low, but the use of surfactants increases it to an average value.

### 3.3. Mechanical Properties of Composites

After matrix characterization, this section is presenting the mechanical properties of the prepared composites with the aforementioned matrices (Table 3) and plain woven carbon fabric (Table 2). Five samples per composite configuration were prepared according to Figure 2.

There is a rather large spread on the results of the stress–strain curves of samples with same composition (Figure 9). This is in part due to the manual production method that limits reproducibility. It is also worth pointing out that some ductile behavior was observed on the failure curves of the composites, as is the aim of making composites. In the first almost linear part, the textile and matrix work together. In the second part, the composite becomes damaged, and delamination or fiber failure can occur. This can be seen, for instance, from the sudden drop in stress. Hence, the prepared composites could be used for engineering applications where some ductility is required, including thin elements and lightweight panels.

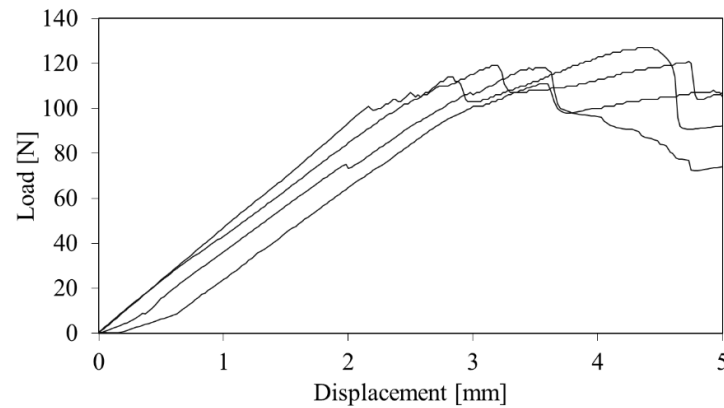


**Figure 9.** Sample of failure curves of composites made of four layers of carbon fiber 200 g/m<sup>2</sup> and five layers of matrix 80K20MK. Measurement on four different samples with the same composition are shown.

The volume fraction of fibers of the composites ranged between 25 to 40 vol% (Figure 10). This wide range is caused by the manual production and the differences in workability of the matrix. Due to the nature of the matrix, it was difficult to achieve composites with more than 40% fiber volume fraction. Considering the fact that flexural strength mainly depends on the fiber properties, because the matrix will crack long before the fibers, the higher the fiber volume fraction, the higher the flexural strength. It is somewhat unfortunate that the addition of MK renders the production of high volume fraction composites more difficult. As a result, these composites have the lowest fiber volume fractions of the series. The fiber volume fraction for the series 80K20MK increased only a bit with surfactants, but remained between 25–30 vol%.

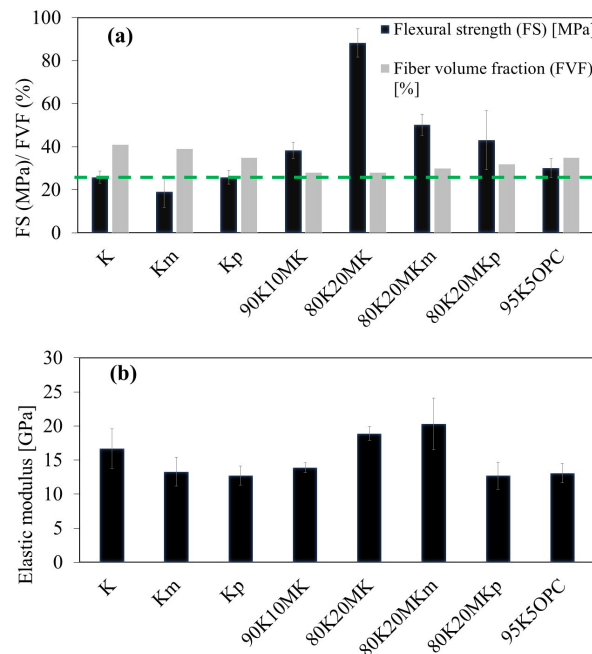


**Figure 10.** Fiber volume fraction, flexural strength (a) and elastic modulus (b) of the respective composites. Names indicate the matrices, as used in Table 3. For each composition, the average of five measurements is given.

Depending on the matrix composition, the flexural strength varied from about 19 to 83 MPa, while the Elastic modulus varied between 13 and 20 GPa (Figure 10). Both the addition of 2-methyl-2,4 pentanediol (Km) and polyethylene glycol (Kp) to Koranel-based matrices had



no or little effect on the flexural strength, and even showed a decrease in the elastic modulus with respect to K (Figure 10). This is in contrast to the increase in the flexural strength and elastic modulus with the surfactant observed in the pure matrices (Figure 8b). The fact that the surfactants do not increase the strength in composites as they do for the pure matrix shows that carbon fiber reinforcement is dominant on the flexural strength and that the difference in matrix properties resulting from surfactant addition did not prevail.

The addition of 10 wt.% of metakaolinite (90K10MK) shows an increase to 40 MPa in flexural strength, but no increase in elastic modulus (5 GPa) with respect to K. Higher performance was observed for samples with 20 wt.% metakaolinite (80K20MK) in the matrix, up to 88 MPa in flexural strength and 20 GPa in elastic modulus. Samples prepared with metakaolinite presented lower fiber volume fraction (25 vol%), but higher mechanical properties than the reference (cf. green dashed line in Figure 10). Hence, the presence of metakaolinite was beneficial for strength development, in consistency with calorimetry results on cumulative heat released (Figure 5). Another reason might be the small particle size of metakaolinite that allows for better contact and maybe even penetration in the textile. The substitution of copper slag by 5 wt.% OPC (95K5OPC) only had a negligible effect on the flexural strength and a decrease in elastic modulus despite the positive effect of OPC on reaction heat.

The flexural strength results are in some cases higher or comparable to the literature values of 40–45 MPa obtained with geopolymer laminate composites prepared with metakaolinite and basalt fabric [12]. These authors also observed that fiber reinforcement favored water evaporation from the composites at room temperature and improved the thermal stability in comparison to the pure matrix when thermally treated at 300–800 °C.

In another study, a bending strength of 18 MPa was observed with blast furnace slag composite reinforced with 1 wt.% of 6 mm long carbon fiber, representing an increase of 19% compared to the pure matrix [37]. Meanwhile, an elastic modulus of 37 GPa and flexural strength of 133 MPa were achieved on potassium-based metakaolin geopolymers with 20–25% volume of unidirectional carbon fiber [38]. The analysis of these results shows some divergences in the bending strength depending on the matrix, fiber type, size and weaving, but in all the cases, the use of fiber was beneficial for the bending strength.

In summary, for the mechanical properties, in comparison to composition K, the surfactant and OPC addition had no or little effect in the studied range of the prepared composites. However, metakaolinite addition had a beneficial effect on the mechanical properties, with about 100% increase in the composite made of matrix containing 20 wt.% MK (Figure 10).

### 3.4. Microstructural Observations

The microstructure of the surface of the composites from compositions K, 80K20MK, 80K20MKm and 80K20MKp is presented in Figure 11. While keeping the same liquid-to-solid ratio, the substitution of Koranel by metakaolinite led to a significant reduction in cracks and composites with smoother surfaces. The addition of both 2-methyl-2,4 pentanediol and polyethylene glycol, however, seemed to increase the void proportion at the surface. This is consistent with a previous study on the use of 2-methyl-2,4 pentanediol, which was observed to lead to an increased porosity by acting as air entrainer with drying shrinkage reduction [23], and may explain why the surfactants do not have a significant effect on the flexural strength and elastic modulus (Figure 10) of the composites. However, the appearance of voids in the samples with surfactants did not significantly influence the density, which was always in the range of  $(2.00 \pm 0.05) \text{ g/cm}^3$ .

The microstructure of the cross section of composite 80K20MK shows alternating layers of matrix and carbon fiber (Figure 12). The matrix is not perfectly adhering to the carbon fiber and is not really penetrating in the fiber bundles. This is ascribed to the fiber's hydrophobic properties, which makes them incompatible with water-based systems [39]. However, methods including plasma treatment, silica or calcite deposition on carbon fiber, were suggested to improve the wettability and enhance the adhesion between the fiber and cementitious matrices [39–42]. Fiber surface chemistry modification and nanomaterials'

incorporation in the binder were also observed to enhance the fiber/matrix interface in alkali-activated composites [43–46]. For instance, the addition of 2 wt.% nano titanium dioxide in alkali-activated fly ash reinforced by micro carbon fiber was observed to increase the fracture toughness by 29% in comparison to the control sample, due to possible filling behavior and enhancement of the carbon fiber–matrix interfacial zone, which induced a hindrance to crack formation [46]. However, actions to improve fiber–matrix interactions are also costly, so need to be analyzed considering the possible improvement in properties and the composite application. Since in this paper the focus is on proving that the matrix can be used for textile-reinforced composites, no effort was exerted to improve the fiber–matrix interaction. Anyway, it is worth reminding that the durability of textile-reinforced alkali-activated composites do not only depend on their resistance to the external environment, but also on the chemical interaction between the fibers and binder within the composite. For instance, due to the alkaline environment of the binder, alkali-activated composites reinforced with glass and basalt fibers were found to have significant reductions in tensile strength their over time, while the strengths of those reinforced with carbon fibers were sufficiently stable [26,47].

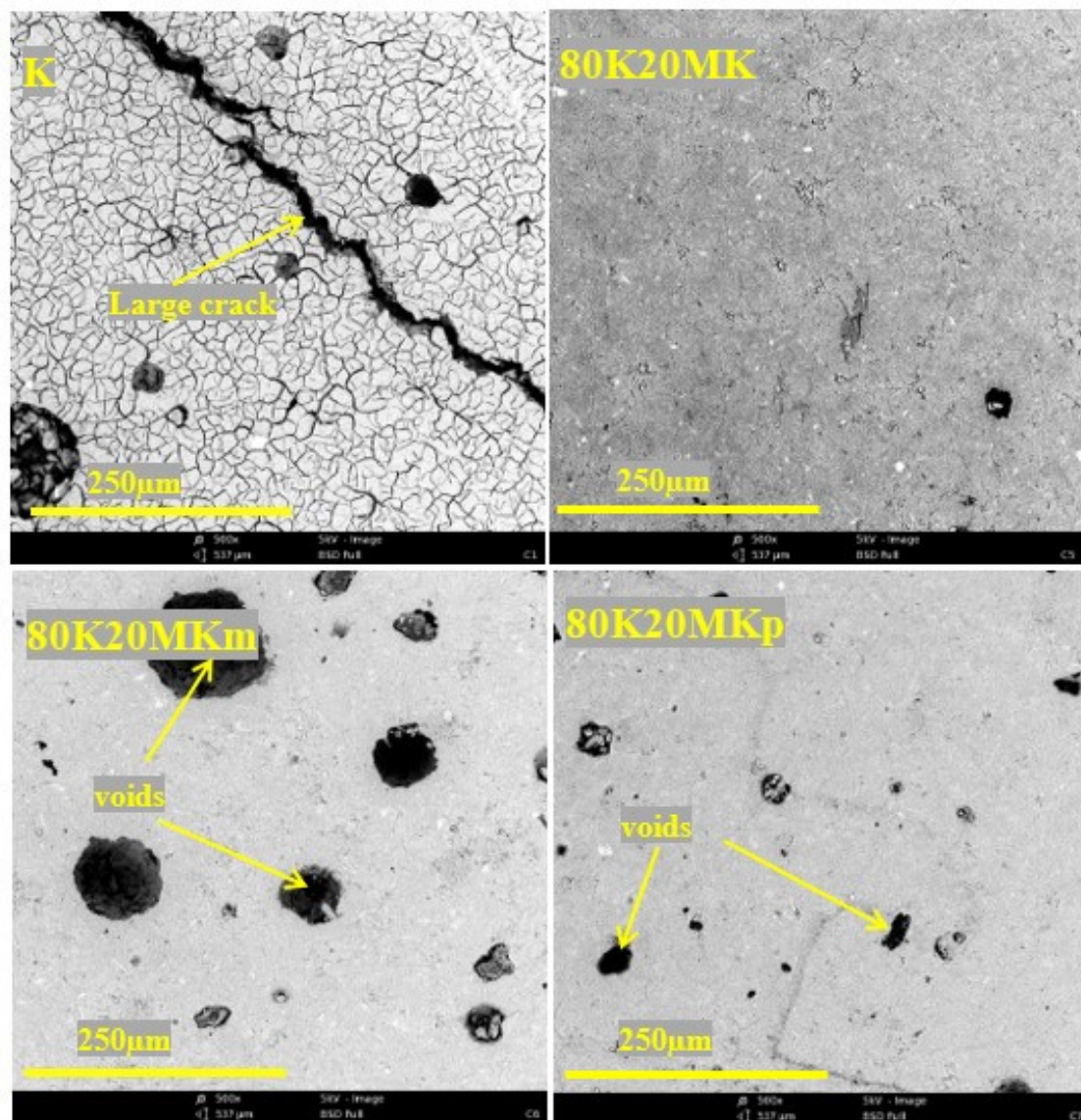


**Figure 11.** Microstructural surface of indicated composites (K), (80K20MK), (80K20MKm) and (80K20MKp) (cf. Table 3).

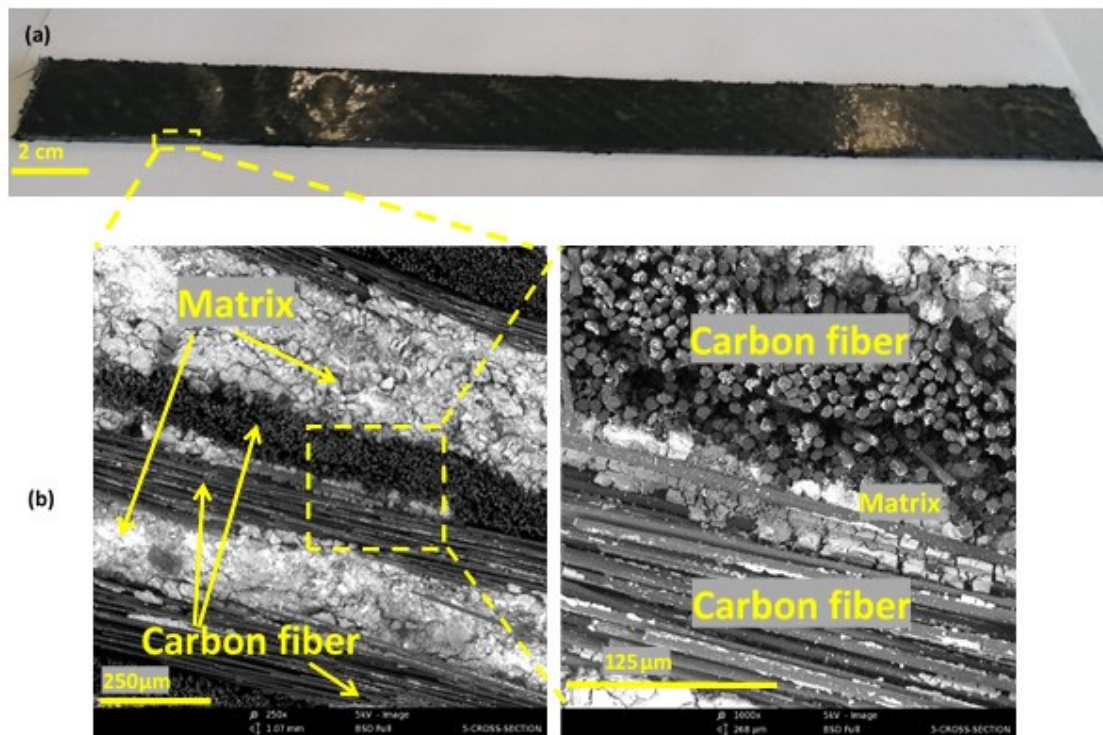


**Figure 12.** (a) photo of the composite; (b) microstructural cross section of laminate composite made of woven carbon fiber and matrix 80K20MK.

### 3.5. Thermal Stability of the Composites

The elastic modulus of the composite and matrix when heating until 700 °C, monitored via impulse excitation, is presented in Figure 13. The elastic modulus of the matrix first decreased from about 5 to 2 GPa, and from about 20 to 250 °C. Then, an increase was observed until around 620 °C, where it reached a value of 9.5 GPa before starting to decrease until it reached 7 GPa at 700 °C. The modulus continued to decrease during the dwell time to 5 GPa and remained almost constant on cooling. The decrease in the elastic modulus of the matrix from 20 to 300 °C occurs in two steps and may be ascribed to microcrack formation due to residual water loss on heating. The first step, around 100 °C, is broad while the second step is more pronounced. The E modulus of the composite has a comparable profile of reduction until about 200 °C. However, for the pure matrix, the decrease is more than 50% up to 250 °C, while for the composite, it is only about 25%. In part, it is due to the reduced amount of matrix because of the fibers in the composite. However, there is only about 25–30 vol% of fibers; thus, this cannot explain the large difference. The effect must thus be linked to reduced cracking, because fibers stop the crack propagation and the interaction between fibers and matrix, reducing the importance of the matrix. Before 300 °C, the elastic moduli of the matrix and composite start to increase, but above 300 °C, the one for the composite decreases again. The most probable explanation for the increase is that the system starts to heal as a result of mobility increase with temperature, although a glass transition could not be observed with calorimetry in this temperature range. The modulus keeps on increasing up to about 630 °C after which it decreases again. A similar behavior was observed in laterite-based alkali-activated materials, where a strength increase was observed on heating between 250 and 450 °C [48]. One should however be aware that the strength does not necessarily follow the same trend as the modulus, because the elongation at failure can be different. The composite, however, shows a reduction in modulus in two steps above 300 °C. The first is probably due to the thermal incompatibility between the matrix and the fiber that led to deterioration upon heating [49]. The second one is at least in part related to the decomposition of the carbon fibers in air. The elastic modulus signal could not be recorded above 640 °C due to sample



deterioration upon heating. The reduction in the mechanical properties upon heating is in line with some reported studies on alkali-activated fiber-reinforced composites [12]. However, some studies also reported an increase in strength when metakaolin geopolymer with carbon fiber reinforcement was heated at 1100–1300 °C, due to matrix crystallization and densification that led to an enhancement of the fiber/matrix-bonding interface [38].

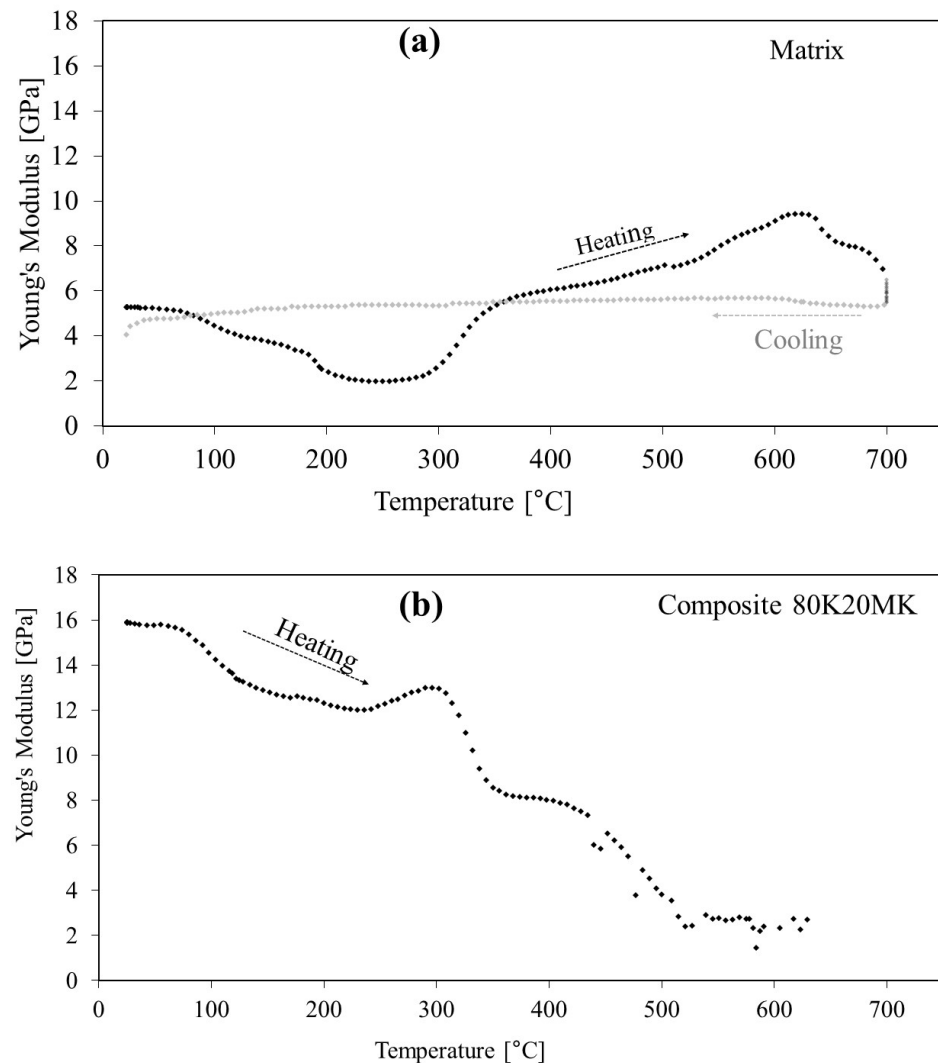


**Figure 13.** Elastic modulus vs. temperature of (a) the matrix and (b) composite 80K20MK.

#### 4. Conclusions

Copper slag is an industrial residue with a large unutilized fraction. The present study investigated the development of alkali-activated composites from copper slag named Koranel and carbon textile-woven fabric. In the first step, the matrix for the composites was developed. The reactivity of Koranel with potassium silicate solutions, with molar ratio  $R = \text{SiO}_2/\text{K}_2\text{O}$  varying from 1 to 2.75 at 0.25 intervals, was investigated using isothermal calorimetry. The results showed that the solution with  $R = 2.0$  has an open pot life of only a few hours at room temperature, while the solution with  $R = 2.25$  has an open pot life of several days at room temperature, but reacts quickly at 80 °C. Hence, the potassium silicate solution with the silica modulus of 2.25 is more suitable for a process in which the composite is impregnated, and in the following hours, would be used for making a laminated composite. The substitution of 5% and 10–20 wt.% Koranel, respectively, by OPC and metakaolinite, led to higher reaction heat. However, higher mechanical strength, especially in flexion, was only observed when 20 wt.% Koranel was substituted by metakaolinite. Meanwhile, OPC addition of only 5 wt.% induced a fast setting of the matrix,

which was not deemed suitable for composite preparation. The effect of the 2 surfactants, 2-methyl 2,4 pentanediol and polyethylene glycol on the workability is limited, but PEG further increased the flexural strength.

Composites were made of four layers of carbon fabric and five layers of inorganic polymer matrix. Pure Koranel-based matrix presented a compressive and flexural strength of about 30–35 MPa and 1–5 MPa, respectively. An improvement in the bending strength was observed with a fiber addition in the prepared composites, with flexural strength values reaching 83 MPa. The addition of 2 wt.% polyethylene glycol/2-methyl 2,4 pentanediol was beneficial for the flexural strength of pure matrix, but the same was not observed in the mechanical properties of the composites.

The microstructure of the cross section showed alternating layers of matrix and carbon fiber, even though the matrix was not perfectly adhering on the carbon fiber and little to no impregnation of the fiber bundles was observed. The E modulus of pure matrix dropped by 50% above 200 °C. The pure matrix healed from 300 °C onwards, and its E modulus reached a maximum at 630 °C, after which it decreases again. At 700 °C, the modulus was about 5 GPa, and remained almost constant upon cooling. The composites have a modulus about 3 times higher at room temperature and lose only 25% of it up to 250 °C. Above 300 °C however, the modulus of the composite gradually decreases. The composite prepared with 20 wt.% metakaolinite still retained 50% of its elastic modulus on heating until 400 °C. However, upon further heating, the modulus decreases to almost 0 at 640 °C.

The results are interesting for the repurposing of Koranel copper slag in the development of alkali-activated composites for various engineering applications, including high strength lightweight panels and laminates. There are several aspects that need further investigation, such as the fiber–matrix interaction, the better impregnation of the fiber bundles, the thermal behavior of the matrix and composites, and the different processes responsible for deterioration and healing. All these aspects will be dealt with in future research.

**Author Contributions:** Conceptualization, P.N.L. and H.R.; Methodology, P.N.L., G.M.H., N.D., J.G. and H.R.; Formal analysis, G.M.H., F.K. and J.G.; Investigation, G.M.H. and F.K.; Data curation, G.M.H. and F.K.; Writing—original draft, P.N.L., G.M.H. and N.D.; Writing—review & editing, P.N.L., G.M.H., N.D., J.G. and H.R.; Supervision, H.R.; Project administration, H.R.; Funding acquisition, H.R. All authors have read and agreed to the published version of the manuscript.

**Funding:** This work was performed in the framework of STIF (ICON, supported by SIM, Flanders, N° HBC.2019.0120). The project has received funding from the European Union’s Horizon 2020 research and innovation programme under N° 963603 Current Direct.

**Institutional Review Board Statement:** Not applicable.

**Informed Consent Statement:** Not applicable.

**Data Availability Statement:** The data presented in this study are available on request from the corresponding author.

**Acknowledgments:** This work was performed in the framework of STIF (ICON, supported by SIM, Flanders, N° HBC.2019.0120). The project has received funding from the European Union’s Horizon 2020 research and innovation programme under N° 963603 Current Direct. The Authors also acknowledged the support from the Department Mechanics of Materials and Constructions (MeMC) of VUB for assistance in mechanical testing.

**Conflicts of Interest:** Author Nicole Dilissen is employed by Buildwise. The remaining authors declare that the research was conducted in the absence of any commercial or financial relationships that could be construed as a potential conflict of interest.

## References

1. Brameshuber, W. *Report 36: Textile Reinforced Concrete-State-of-the-Art Report of RILEM TC 201-TRC*; RILEM Publications: Trondheim, Norway, 2006; Volume 36, ISBN 2-912143-99-3.
2. Li, Y.; Yin, S.; Lv, H. Combined effects of dry-wet cycles and sustained loads on the seismic behavior of TRC-strengthened RC columns. *Structures* **2021**, *33*, 2226–2237. [[CrossRef](#)]



3. Mechtcherine, V.; Schneider, K.; Brameshuber, W. 2—Mineral-based matrices for textile-reinforced concrete. In *Textile Fibre Composites in Civil Engineering*; Triantafyllou, T., Ed.; Woodhead Publishing: Sawston, UK, 2016; pp. 25–43; ISBN 978-1-78242-446-8.
4. Ospitia, N.; Tsangouri, E.; Pourkazemi, A.; Stiens, J.H.; Aggelis, D.G. NDT inspection on TRC and precast concrete sandwich panels: A review. *Constr. Build. Mater.* **2021**, *296*, 123622. [[CrossRef](#)]
5. Van Driessche, A.; Aggelis, D.G.; Tsangouri, E. Complex fracture on thin-wall textile reinforced cement (TRC) shells monitored by acoustic emission. *Thin-Walled Struct.* **2021**, *167*, 108216. [[CrossRef](#)]
6. Mohan, A.; Madhavi, T.C. Development of binders for textile reinforced concrete. *Mater. Today Proc.* **2021**, *46*, 3297–3301. [[CrossRef](#)]
7. Tekle, B.H.; Messerer, D.; Holschemacher, K. Bond induced concrete splitting failure in textile-reinforced fine-grained concrete. *Constr. Build. Mater.* **2021**, *303*, 124503. [[CrossRef](#)]
8. Alzeer, M.I.M.; MacKenzie, K.J.D. Chapter 5—Fiber composites of inorganic polymers (geopolymers) reinforced with natural fibers. In *Composite Materials*; Low, I.-M., Dong, Y., Eds.; Elsevier: Amsterdam, The Netherlands, 2021; pp. 117–147; ISBN 978-0-12-820512-9.
9. Naaman, A.E. 18—Thin TRC products: Status, outlook, and future directions. In *Textile Fibre Composites in Civil Engineering*; Triantafyllou, T., Ed.; Woodhead Publishing: Sawston, UK, 2016; pp. 413–439; ISBN 978-1-78242-446-8.
10. Valeri, P.; Fernández Ruiz, M.; Muttoni, A. Tensile response of textile reinforced concrete. *Constr. Build. Mater.* **2020**, *258*, 119517. [[CrossRef](#)]
11. Alomayri, T.; Shaikh, F.U.A.; Low, I.M. Synthesis and mechanical properties of cotton fabric reinforced geopolymer composites. *Compos. Part B Eng.* **2014**, *60*, 36–42. [[CrossRef](#)]
12. Ribero, D.; Kriven, W.M. Properties of Geopolymer Composites Reinforced with Basalt Chopped Strand Mat or Woven Fabric. *J. Am. Ceram. Soc.* **2016**, *99*, 1192–1199. [[CrossRef](#)]
13. Samal, S.; Marvalová, B.; Petříková, I.; Vallons, K.A.M.; Lomov, S.V.; Rahier, H. Impact and post impact behavior of fabric reinforced geopolymer composite. *Constr. Build. Mater.* **2016**, *127*, 111–124. [[CrossRef](#)]
14. Peys, A.; White, C.E.; Rahier, H.; Blanpain, B.; Pontikes, Y. Alkali-activation of CaO-FeOx-SiO<sub>2</sub> slag: Formation mechanism from in-situ X-ray total scattering. *Cem. Concr. Res.* **2019**, *122*, 179–188. [[CrossRef](#)]
15. Provis, J.L.; van Deventer, J.S.J. *Alkali Activated Materials State-of-the-Art Report, RILEM TC 224-AAM*; Springer: Dordrecht, The Netherlands, 2014; ISBN 978-94-007-7672-2.
16. Flesoura, G.; Dilissen, N.; Dimitrakis, G.; Vleugels, J.; Pontikes, Y. A new approach for the vitrification of municipal solid waste incinerator bottom ash by microwave irradiation. *J. Clean. Prod.* **2021**, *284*, 124787. [[CrossRef](#)]
17. Van De Sande, J.; Peys, A.; Hertel, T.; Rahier, H.; Pontikes, Y. Upcycling of non-ferrous metallurgy slags: Identifying the most reactive slag for inorganic polymer construction materials. *Resour. Conserv. Recycl.* **2020**, *154*, 104627. [[CrossRef](#)]
18. Lemougna, P.N.; Yliniemi, J.; Adesanya, E.; Tanskanen, P.; Kinnunen, P.; Roning, J.; Illikainen, M. Reuse of copper slag in high-strength building ceramics containing spodumene tailings as fluxing agent. *Miner. Eng.* **2020**, *155*, 106448. [[CrossRef](#)]
19. Siddique, R.; Singh, M.; Jain, M. Recycling copper slag in steel fibre concrete for sustainable construction. *J. Clean. Prod.* **2020**, *271*, 122559. [[CrossRef](#)]
20. Saidi, M.; Reboul, N.; Gabor, A. Cyclic behaviour of textile-reinforced cementitious matrix composites (TRC) using distributed fibre optic sensors technology. *Compos. Part Appl. Sci. Manuf.* **2021**, *149*, 106531. [[CrossRef](#)]
21. Shen, L.; Wang, J.; Xu, S.; Zhao, X.; Peng, Y. Flexural behavior of TRC contained chopped fibers subjected to high temperature. *Constr. Build. Mater.* **2020**, *262*, 120562. [[CrossRef](#)]
22. Yin, S.; Cong, X.; Wang, C.; Wang, C. Research on flexural performance of composited RC beams with different forms of TRC permanent formwork. *Structures* **2021**, *29*, 1424–1434. [[CrossRef](#)]
23. Beersaerts, G.; Ascensão, G.; Pontikes, Y. Modifying the pore size distribution in Fe-rich inorganic polymer mortars: An effective shrinkage mitigation strategy. *Cem. Concr. Res.* **2021**, *141*, 106330. [[CrossRef](#)]
24. *EN 196-6:2018*; Methods of testing cement—Part 6: Determination of fineness. EN: Plzen, Czech Republic, 2018.
25. Lemougna, P.N.; Dilissen, N.; Hernandez, G.M.; Kingne, F.; Gu, J.; Rahier, H. Effect of Sodium Disilicate and Metasilicate on the Microstructure and Mechanical Properties of One-Part Alkali-Activated Copper Slag/Ground Granulated Blast Furnace Slag. *Materials* **2021**, *14*, 5505. [[CrossRef](#)]
26. Ranjbar, N.; Zhang, M. Fiber-reinforced geopolymer composites: A review. *Cem. Concr. Compos.* **2020**, *107*, 103498. [[CrossRef](#)]
27. De Baere, L.; Van Paepegem, W.; Degrieck, J.; Sol, H.; Van Hemelrijck, D.; Petreli, A. Comparison of different identification techniques for measurement of quasi-zero Poisson's ratio of fabric-reinforced laminates. *Compos. Part Appl. Sci. Manuf.* **2007**, *38*, 2047–2054. [[CrossRef](#)]
28. Messiry, M.E. Theoretical analysis of natural fiber volume fraction of reinforced composites. *Alex. Eng. J.* **2013**, *52*, 301–306. [[CrossRef](#)]
29. Kriskova, L.; Machiels, L.; Pontikes, Y. Inorganic Polymers from a Plasma Converter Slag: Effect of Activating Solution on Microstructure and Properties. *J. Sustain. Metall.* **2015**, *1*, 240–251. [[CrossRef](#)]
30. Onisei, S.; Lesage, K.; Blanpain, B.; Pontikes, Y. Early Age Microstructural Transformations of an Inorganic Polymer Made of Fayalite Slag. *J. Am. Ceram. Soc.* **2015**, *98*, 2269–2277. [[CrossRef](#)]
31. Yao, X.; Zhang, Z.; Zhu, H.; Chen, Y. Geopolymerization process of alkali–metakaolinite characterized by isothermal calorimetry. *Thermochim. Acta* **2009**, *493*, 49–54. [[CrossRef](#)]

32. Caron, R.; Patel, R.A.; Dehn, F. Activation kinetic model and mechanisms for alkali-activated slag cements. *Constr. Build. Mater.* **2022**, *323*, 126577. [[CrossRef](#)]
33. Rahier, H.; Van Mele, B.; Biesemans, M.; Wastiels, J.; Wu, X. Low-temperature synthesized aluminosilicate glasses. *J. Mater. Sci.* **1996**, *31*, 71–79. [[CrossRef](#)]
34. Peys, A.; White, C.E.; Olds, D.; Rahier, H.; Blanpain, B.; Pontikes, Y. Molecular structure of CaO–FeO<sub>x</sub>–SiO<sub>2</sub> glassy slags and resultant inorganic polymer binders. *J. Am. Ceram. Soc.* **2018**, *101*, 5846–5857. [[CrossRef](#)]
35. Luukkonen, T.; Abdollahnejad, Z.; Yliniemi, J.; Kinnunen, P.; Illikainen, M. One-part alkali-activated materials: A review. *Cem. Concr. Res.* **2018**, *103*, 21–34. [[CrossRef](#)]
36. Suda, V.B.R.; Priyatham Paul, S. Relationship between compressive, split tensile and flexural strengths of ternary blended concrete. *Int. Conf. Adv. Constr. Mater. Struct.* **2022**, *65*, 1112–1119. [[CrossRef](#)]
37. Vilaplana, J.L.; Baeza, F.J.; Galao, O.; Alcocel, E.G.; Zornoza, E.; Garcés, P. Mechanical properties of alkali activated blast furnace slag pastes reinforced with carbon fibers. *Constr. Build. Mater.* **2016**, *116*, 63–71. [[CrossRef](#)]
38. He, P.; Jia, D.; Lin, T.; Wang, M.; Zhou, Y. Effects of high-temperature heat treatment on the mechanical properties of unidirectional carbon fiber reinforced geopolymer composites. *Ceram. Int.* **2010**, *36*, 1447–1453. [[CrossRef](#)]
39. Mechtcherine, V.; Michel, A.; Liebscher, M.; Schneider, K.; Großmann, C. Mineral-impregnated carbon fiber composites as novel reinforcement for concrete construction: Material and automation perspectives. *Autom. Constr.* **2020**, *110*, 103002. [[CrossRef](#)]
40. Li, H.; Liebscher, M.; Ranjbarian, M.; Hempel, S.; Tzounis, L.; Schröfl, C.; Mechtcherine, V. Electrochemical modification of carbon fiber yarns in cementitious pore solution for an enhanced interaction towards concrete matrices. *Appl. Surf. Sci.* **2019**, *487*, 52–58. [[CrossRef](#)]
41. Lu, M.; Xiao, H.; Liu, M.; Li, X.; Li, H.; Sun, L. Improved interfacial strength of SiO<sub>2</sub> coated carbon fiber in cement matrix. *Cem. Concr. Compos.* **2018**, *91*, 21–28. [[CrossRef](#)]
42. Raphael, N.; Namratha, K.; Chandrashekar, B.N.; Sadasivuni, K.K.; Ponnamma, D.; Smitha, A.S.; Krishnaveni, S.; Cheng, C.; Byrappa, K. Surface modification and grafting of carbon fibers: A route to better interface. *Prog. Cryst. Growth Charact. Mater.* **2018**, *64*, 75–101. [[CrossRef](#)]
43. Růžek, V.; Dostayeva, A.M.; Walter, J.; Grab, T.; Korniejenko, K. Carbon Fiber-Reinforced Geopolymer Composites: A Review. *Fibers* **2023**, *11*, 17. [[CrossRef](#)]
44. Rahman, A.S.; Jackson, P.; Radford, D.W. Improved toughness and delamination resistance in continuous fiber reinforced geopolymer composites via incorporation of nano-fillers. *Cem. Concr. Compos.* **2020**, *108*, 103496. [[CrossRef](#)]
45. Huang, L.; Tang, L.; Bachinger, A.; Li, Y.; Yang, Z. Improving the performance of alkali-activated slag mortar with electro/chemically treated carbon fiber textile. *J. Clean. Prod.* **2023**, *418*, 138214. [[CrossRef](#)]
46. Raza, A.; Azab, M.; Baki, Z.A.; El Hachem, C.; El Ouni, M.H.; Kahla, N.B. Experimental study on mechanical, toughness and microstructural characteristics of micro-carbon fibre-reinforced geopolymer having nano TiO<sub>2</sub>. *Alex. Eng. J.* **2023**, *64*, 451–463. [[CrossRef](#)]
47. Funke, H.; Gelbrich, S.; Kroll, L. The Durability and Performance of Short Fibers for a Newly Developed Alkali-Activated Binder. *Fibers* **2016**, *4*, 11. [[CrossRef](#)]
48. Lemougna, P.N.; Madi, A.B.; Kamseu, E.; Melo, U.C.; Delpiancke, M.-P.; Rahier, H. Influence of the processing temperature on the compressive strength of Na activated lateritic soil for building applications. *Constr. Build. Mater.* **2014**, *65*, 60–66. [[CrossRef](#)]
49. Behera, P.; Baheti, V.; Militky, J.; Louda, P. Elevated temperature properties of basalt microfibril filled geopolymer composites. *Constr. Build. Mater.* **2018**, *163*, 850–860. [[CrossRef](#)]

**Disclaimer/Publisher’s Note:** The statements, opinions and data contained in all publications are solely those of the individual author(s) and contributor(s) and not of MDPI and/or the editor(s). MDPI and/or the editor(s) disclaim responsibility for any injury to people or property resulting from any ideas, methods, instructions or products referred to in the content.